Journal of Great Lakes Research 41 (2015) 607–617

Contents lists available at ScienceDirect

Journal of Great Lakes Research

journal homepage: www.elsevier.com/locate/jglr

Sediment accumulation rates and sediment dynamics using five different methods in a well-constrained impoundment: Case study from Union Lake, Michigan

M. Baskaran [a,*], C.J. Miller [b], A. Kumar [a], E. Andersen [b], J. Hui [b], J.P. Selegean [c], C.T. Creech [c], J. Barkach [d]

[a] Department of Geology, Wayne State University, Detroit, MI 48202, USA
[b] Department of Civil and Environmental Engineering, Wayne State University, Detroit, MI 48202, USA
[c] U.S. Army Corps of Engineers, Detroit, MI 48226, USA
[d] Great Lakes Environmental Center Inc., Farmington Hills, MI 48334, USA

ARTICLE INFO

Article history:
Received 27 March 2014
Accepted 19 January 2015
Available online 7 April 2015

Communicated by Gerald Matisoff

Index words:
Reservoir sedimentation
Pb-210 dating
Sediment retention
Cs-137 dating

ABSTRACT

The single most important factor affecting the longevity of US dams is sedimentation, reducing and perhaps eliminating the reservoir capacity for future sediment storage and flood wave attenuation. A better understanding of the sedimentation rates and sediment dynamics is required for a better management of these dams. Towards this, we collected and analyzed 7 sediment cores from Union Lake for excess ^{210}Pb and ^{137}Cs to determine the sediment accumulation rates ($^{210}Pb_{xs}$-based: 0.12 to 0.28 g cm^{-2} y^{-1}; peak ^{137}Cs-based: 0.13 to 0.29 g cm^{-2} y^{-1}). These average sediment accumulation rates obtained using radionuclides are compared with three other methods: i) bathymetry-based, from the cumulative mass depth of the core and age of the impoundment (0.09 to 0.26 g cm^{-2} y^{-1}); ii) sediment-yield curve obtained for 61 other watersheds (1.2 g cm^{-2} y^{-1}); and iii) gage data of sediment discharge (0.21 g cm^{-2} y^{-1}). Such a comparison provides insight on refining the sediment-yield curve-based sediment loading in the impoundment. Vertical profiles of ^{137}Cs provide not only insight on sediment mixing (based on a novel method by analyzing the Gaussian-like curve), but also the effectiveness of vibra-coring method in retrieving the full length of the soft sediment deposited since the construction of the dam. The present investigation can serve as a model study for application to other dams in the Great Lakes region and has implications to larges lakes in the Great Lakes catchment for the prediction of sediment accumulation rates using a variety of methods.

Introduction

A major threat to the productivity and longevity of a majority of the aging dams in the mid-western United States is the rate of sedimentation. The trapping efficiency of many of the reservoirs is unknown, but according to the World Bank, it is estimated that average reservoirs around the world are losing about 1% of storage per year due to sedimentation (World Bank, 1998). It is estimated that more than 85% of the large dams (height >15 m from the foundation with a reservoir volume of >3 × 10^6 m^3) in the continental United States will be more than 50 y old by 2020 (Hossain et al., 2009) and a major portion of these dams are reaching near their capacity in terms of sediment storage. The larger dams have the potential to vastly change local climate, landscapes, urbanization patterns and local and regional economics (Hossain et al., 2009). Construction or removal of larger dams not only has direct impact on the large scale land use and land cover changes, but also their potential loss could aggravate extreme weather patterns. The vertical temperature and humidity profiles due to evaporation of water above large dams could even alter the local atmospheric instabilities due to changes in surface fluxes of heat and moisture. Concerns have been raised on whether these aging structures can withstand the extreme accelerated climate change in the near future.

Watershed land use changes, including urbanization, are expected to have resulted in accelerated soil erosion and sediment accumulation rates. The impacts of sedimentation in reservoirs have been investigated using site assessment techniques, physical and mathematical modeling and sediment accumulation and mixing rate studies using short-lived radionuclides (e.g., ^{210}Pb, ^{137}Cs, ^{7}Be, ^{234}Th). These radionuclides can also serve as powerful tools in the investigation of sediment depositional and erosional patterns, as well as tracers to identify sediment transport processes during flood events.

There are a number of techniques to determine the post-construction sediment loading to a reservoir. These include the use of: i) measured $^{210}Pb_{xs}$, ^{137}Cs or ^{239,240}Pu vertical profiles; ii) measured bathymetry at multiple post-construction sites; iii) sediment transport modeling; and iv) data from upstream sediment gages. In this manuscript, we present a comparison of sediment accumulation rates (SAR) obtained by these four methods in Union Lake, an impoundment constructed in 1923, in

* Corresponding author.
E-mail address: Baskaran@wayne.edu (M. Baskaran).

http://dx.doi.org/10.1016/j.jglr.2015.03.013
0380-1330/

Michigan, USA. We also identify the flood deposits based on vertical $^{210}Pb_{xs}$ and ^{226}Ra profiles, validating this historical marker method.

Relevance of this study to the Laurentian Great Lakes

The sediment retention characteristics in Union Lake have relevance to the hundreds of small reservoirs in the Great Lakes watershed which in turn can impact the sediment delivery to the Great Lakes. The removal of these reservoirs will result in a significant increase in sediment delivery to the Great Lakes. The effective utility ^{210}Pb and ^{137}Cs as geochronometer for dating sediments can be well-constrained in smaller and constructed impoundment in the time scale where these nuclides are useful. For example, validation of the $^{210}Pb_{xs}$ and ^{137}Cs-based chronology with the total depth of the core is only possible, when the age of the lake is comparable to the time-range covered by the isotope used. In the present study, ^{210}Pb age range goes to ~100 y and ^{137}Cs goes back to ~60 y before present. Because the reservoir age is known, this study is ideal to compare the $^{210}Pb_{xs}$ and ^{137}Cs-based chronologies with those obtained from three other methods (sediment-yield curve, gage data of sediment discharge and total length of the curve) of which the absolute method is the one based on the total length of the core. Inter-comparison of different dating methods has direct relevance to dating of sediments over ~100 y time scale in large lakes around the globe.

Materials and methods

Study area description

Riley Dam was constructed in 1923, forming the associated impoundment of Union Lake. Prior to 1923, the St. Joseph River meandered through the current impounded area on the north side of Union Lake (Fig. 1). Riley Dam impounds Union Lake in Branch County, Michigan and is located in the St. Joseph River basin on the main branch of the St. Joseph River, just downstream of Union City, Michigan (Fig. 1). The Union Lake subwatershed area consisted primarily of forest as well as wetland and savanna prior to the construction of the impoundment (Comer and Albert, 1998). The original reservoir floor before construction consisted of sand- and gravel-sized glacial till, with the silt–clay sediments overlying this material. The sediment trapping efficiency in Union Lake is unknown; however, the reduction in sediment delivery to downstream seems significant (Creech et al., 2010). The impounded lake has a surface area of 2.12×10^6 m^2 (= 525 acres), and a storage volume of 4.00×10^6 m^3 (= 3240 acre-feet; National Inventory of Dams, 2010). Changing land use dynamics can be assessed using the population growth in the 3 counties (Calhoun, Hillsdale and Branch) in portions of the Union Lake subwatershed. The population growth of 81% from 127,138 in 1920 to 230,299 in 2000 has resulted in significant changes in the land use in the watershed (Creech et al., 2010).

Field sampling

Bathymetry of the Union Lake is given in Fig. 1. A total of thirteen sediment cores (7 cores analyzed for radionuclides are only shown in Fig. 1 and the rest of the cores were collected too close to the cores that we analyzed to place in Fig. 1) were collected in July 2010 from different localities along the dam, representing the whole water depth (maximum water depth: 5 m; 4–5 m: 1 core; 3–4 m: 1 core; 2–3 m: 3 cores; 1–2 m: 2 cores), with a vibra-coring unit onboard a boat, from the river delta to the impoundment (Fig. 1). The acetate butyrate core tubes (inside diameter of 10 cm) were transported vertically to the laboratory where they were frozen to prevent disturbance or loss of

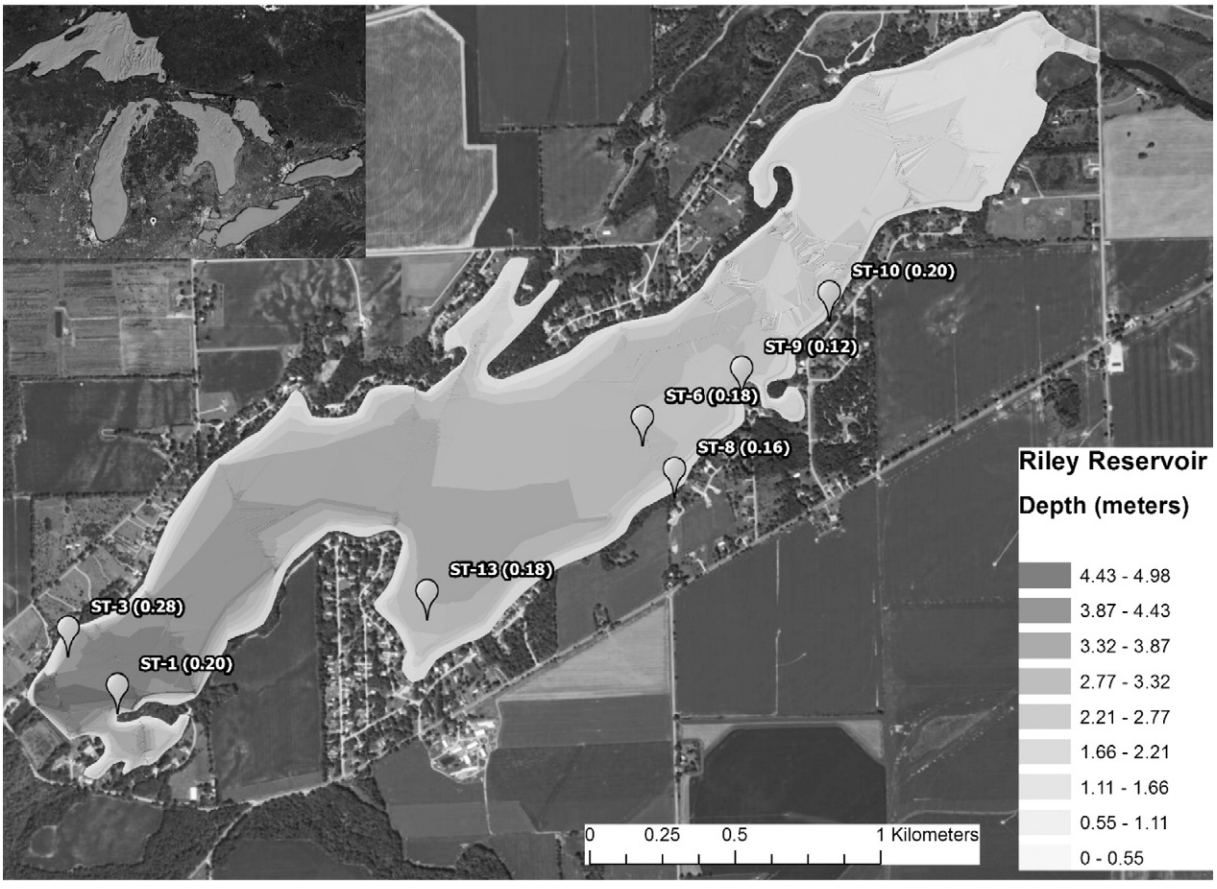

Fig. 1. Station number of sample location (numbers in parenthesis denote sediment accumulation rate based on $^{210}Pb_{xs}$ vertical profile) in a Bathymetric map of Union Lake, Michigan. Latitude and longitude are given in Table 1.

material. It is possible that there was compaction of sediments from the time of retrieval to the time of storage in the laboratory.

The sediment cores were sliced into 1 cm thick layers in the upper 10 cm and subsequently at 2 cm intervals the rest of the cores. Although no noticeable varves were observed, it is anticipated that most river-borne coarse-grained sedimentary materials are expected to have been trapped in the relatively flat upstream region of the dam. In each section, the outer layer was shaved-off and discarded to minimize contamination. Each cut section was homogenized, and ~ 1/3 of the mixed sediments were utilized for radionuclide analysis. The mixed sediment layers were weighed prior to and after drying at ~85 °C. From the wet and dry weight of the sediment, sediment layer water content was determined. From the water content, porosity (ϕ) for each section was determined from the following equation:

$$\phi = \frac{f_w}{(f_w + (1-f_w)\rho_w/\rho_s)} \quad (1)$$

where f_w is the fraction of water in the wet sediments $\left(= 1 - \frac{\text{dry wt}}{\text{wet wt}}\right)$, ρ_w is the density of pore water (assumed to be 1 g cm^{-3}), and ρ_s is the density of dry solids (assumed to be 2.5 g cm^{-3}).

The cumulative mass depths (M in g cm^{-2}) for sediment cores were calculated from the following equation:

$$M = \sum_I ((1-\phi_i) \times \rho_s \times \delta_x) \quad (2)$$

where ϕ_i is the porosity of the '*i*' section and δ_x is the thickness of each interval (1 or 2 cm).

Laboratory analyses

^{210}Pb activities were determined from the measured activities of ^{210}Po by alpha spectrometry by assuming that ^{210}Po and ^{210}Pb were in secular equilibrium. Details on sediment digestion, and electroplating of Po on to Ag planchets are given in Jweda (2008) and Jweda and Baskaran (2011). Briefly, about 1.5 g of dried and pulverized sample was taken in 120 mL PFA (Savillex) digestion vessel and added 0.75 mL of ^{209}Po spike (8.09 ± 0.02 dpm mL^{-1}). To this mixture, 10 mL each of concentrated HF, HNO_3, and HCl was added and the sample was digested for 24 h at 90 °C. After the digestion is complete, the digested solution was dried in a hot plate and added 5 mL 6 M HCl and dried twice. Finally, the residue was taken in 5 mL 6 M HCl and diluted with 5 mL of deionized water. The pH was adjusted to 2.0 by addition of ammonium hydroxide and iron and other oxidants were reduced by the addition of 0.20 g of ascorbic acid. Polonium was plated by spontaneous deposition onto silver planchets (Jweda, 2008) and was analyzed by an alpha spectrometer with a surface barrier detector coupled to an Octete-PC (ORTEC Co.).

For the measurement of gamma-emitting radionuclides, ~10–15 g of dried pulverized sediments was packed into 10 mL counting vials and assayed. The activities of ^{226}Ra and ^{137}Cs were measured using a high-purity germanium well detector coupled to a Canberra InSpector multi-channel analyzer. There was no peak background for any of the radionuclides analyzed. The gamma ray detector was calibrated with sediment standards [IAEA-300 for ^{137}Cs (661.6 keV) and RGU-1 for ^{226}Ra (via ^{214}Pb and ^{214}Bi at 352 keV and 609 keV, respectively)] obtained from the International Atomic Energy Agency (IAEA). Typical resolution (full-width at half-maximum) was about ~1.3 keV at 46 keV and ~2.2 keV at 1.33 MeV (Jweda and Baskaran, 2011).

Results

Activities of ^{210}Pb$_{xs}$ and ^{137}Cs

The water depth and total sediment thickness as measured by the length of the vibra-core are given in Table 1. The lengths of the cores varied between 26.7 and 99.1 cm, although some of the vertical profiles of ^{137}Cs indicate that the complete length of the core was not recovered by the vibra-coring device (more details given below). The concentrations of ^{210}Pb, ^{226}Ra and ^{137}Cs in the dated cores are given in Electronic Supplementary Material (ESM) Table S1. The ^{226}Ra concentrations vary between 1.5 and 3.1 dpm/g in 119 out of the 125 split samples (ESM Table S1), with one sample having 5.2 dpm/g, and 5 samples between 1.0 and 1.5 dpm/g. The lowest concentrations in RD-13, RD-10 appear to be due to flooding events corresponding to 1952 when the coarser grain-size sediment loading was higher. Generally, finer sediments (mud fraction, <63 μm) contain higher concentrations of ^{226}Ra while the sand fraction contains generally lower ^{226}Ra activity (Baskaran and Naidu, 1995; Ravichandran et al., 1995).

The concentrations of ^{210}Pb$_{xs}$ in the upper 0–1 cm vary considerably, from 5.1 to 10.4 dpm/g, almost by a factor of 2 (ESM Table S1). The maximum ^{210}Pb$_{xs}$ concentration is found in the upper 2 cm layer in 5 out of the 7 sediment cores dated and in the remaining two cores, it was found subsurface (8.21±0.41 dpm/g at 0–1 cm and 8.54±0.39 dpm/g at 8–9 cm in RD-1; 6.68±0.20 dpm/g at 0–1 cm and 7.27±0.26 dpm/g in 3–4 cm in RD-6). This is in contrast to the observation in other freshwater systems where the highest ^{210}Pb$_{xs}$ were consistently found subsurface (e.g., Robbins et al., 1990; Jweda and Baskaran, 2011) and were attributed to physical/biological mixing processes in the upper surface layers (e.g., Crusius et al., 2004). It appears that the sediment mixing appears to be less of a problem in many of these cores. The ^{137}Cs concentrations in the upper 1 cm layer varied between 0.92 and 1.33 dpm/g, similar to the variations in the activities of ^{210}Pb$_{xs}$ (Fig. 3). All of the ^{137}Cs in the upper layers corresponding to sediments deposited after 1970 are derived either from watershed erosional input or from redistribution of resuspended ^{137}Cs-laden sedimentary particles, as atmospheric deposition of ^{137}Cs is negligible since early 1970s (Ritchie and McHenry, 1990; Fuller et al., 1999). If there is uniform erosional input, then, we would expect near constant concentration in the upper sedimentary layers. However, the variations do indicate that there are other processes (e.g., variable erosional input, variable amounts of dissolved and colloidal ^{137}Cs in the water, physical resuspension of the upper layers) that regulate the ^{137}Cs concentration in the top 1 cm layer. There is no significant correlation between the activities of ^{210}Pb$_{xs}$ and ^{137}Cs in the upper 1 cm of the sediment cores (Fig. 2).

The penetration depths of ^{210}Pb$_{xs}$ and ^{137}Cs, their inventories, and the peak ^{137}Cs depths for all the 7 sediment cores are given in Table 1 (Figs. 3 and 4). Four (Riley-3, 6, 10, 13) of the seven cores clearly indicate a subsurface ^{137}Cs peak and that the activity levels at depth in the cores are below the detection limit (BDL). In the remaining three cores (Riley-1, 8, 9), the layers corresponding to activities BDL were not collected and it is uncertain if the highest measured ^{137}Cs activities correspond to 1963 nuclear fallout peak. The peak ^{137}Cs activities range from 3.24 to 5.38 dpm/g (mean: 3.83 dpm/g) in the 4 cores where the lowest activity is BDL and 1.4 to 3.83 dpm/g in the remaining 3 cores (RD-1: 2.52 dpm/g; RD-8: 3.83 dpm/g; and RD-9: 3.51 dpm/g) where the bottom-most layer had measurable ^{137}Cs activity. The peak ^{137}Cs activities in all the sediment cores where the bottom-most layers had activities BDL are comparable to earlier studies in other freshwater systems in Michigan (e.g., Robbins et al., 1990; Jweda and Baskaran, 2011). From the measured peak ^{137}Cs activity in RD-1, 8, 9 cores, it appears that the peak activity is likely below the bottom-most layer collected. However, we have used the highest activity to correspond to year 1963 for comparing with the ^{210}Pb$_{xs}$-based chronology. Note that the presence/absence of ^{137}Cs activity in bottom-most sediment layer could provide important information as to whether the depth of core is complete or only partial core was retrieved from the coring operation.

The depths below which ^{210}Pb$_{xs}$ and ^{137}Cs were not detected are given in Table 1. In most of the cores, the ^{210}Pb penetration depth exceeds the length of the core, as the total thickness of the sediments only corresponds to the last 87 y and 6.7% of the initial activity deposited 87 y ago is expected to still remain at the bottom-most layer of the core

Table 1
Core number and core sampling depth (m; maximum depth of Union Lake is 5 m), core length, core location, penetration depths (D_i) of ^{137}Cs and ^{210}Pb$_{xs}$, measured inventories of ^{137}Cs (I_m^{Cs})[1] and ^{210}Pb$_{xs}$ (I_m^{Pb}), measured ^{210}Pb$_{xs}$/^{137}Cs inventory ratios, and peak ^{137}Cs depths in sediment cores collected from Union Lake, Michigan. Inventories of ^{137}Cs were corrected to January 1, 2011. Inventories are for ^{137}Cs in cores RD-1, RD-8 and RD-9, do not represent the total inventory for the whole core due to incomplete coring.

Core sample	Core length (cm)	Latitude (N)	Longitude (W)	D_{Cs} (cm)	D_{Pb} (cm)	I_m^{Csa} (dpm cm^{-2})	I_m^{Pbb} (dpm cm^{-2})	Measured inventory ^{210}Pb$_{xs}$/^{137}Cs	Peak ^{137}Cs depth (cm)
RD-1 (4.0)	30	42.04436	85.1995	>30	>30	14.8 ± 0.2 (4.5)	35.6 ± 0.7 (0.71)	2.39	27
RD-3 (3.2)	71	42.04616	85.2015	66	>71	40.0 ± 0.3 (12.2)	82.4 ± 0.8 (1.64)	2.04	49
RD-6 (2.1)	40	42.05231	85.1775	36	>40	17.6 ± 0.2 (5.4)	36.9 ± 0.5 (0.74)	2.09	27
RD-8 (1.7)	20	42.05069	85.1762	>20	>20	18.0 ± 0.2 (5.5)	21.5 ± 0.6 (0.43)	1.19	17
RD-9 (2.1)	24	42.05378	85.1733	>24	>24	18.9 ± 0.2 (5.8)	33.5 ± 0.6 (0.67)	1.77	19
RD-10 (1.6)	40	42.05606	85.1696	32	>40	30.7 ± 0.3 (9.4)	30.5 ± 0.9 (0.61)	0.99	21
RD-13 (2.4)	50	42.04707	85.1866	40	42	23.5 ± 0.2 (7.2)	33.4 ± 0.4 (0.67)	1.40	31

[a] Numbers in parenthesis denote the ratio of measured ^{137}Cs inventory to the estimated overhead fallout-derived inventory of 3.27 dpm cm^{-2}; note that the watershed erosional input is not included in the calculated ratios of the inventories (discussion in the Results section).
[b] Numbers in parenthesis denote the ratio of measured ^{210}Pb$_{xs}$ inventory to the direct atmospheric fallout inventory of 50.2 dpm cm^{-2} (assuming annual depositional flux of 1.56 dpm cm^{-2}); note that the watershed erosional input is not included in the calculated the ratios of the inventories (discussion in the Results section).

(pre-construction time). In four cores, the ^{137}Cs activities reach below detection limit. Using the peak ^{137}Cs activity, the calculated SARs are given in Table 2. Using this SAR and the peak ^{137}Cs layer, the layer corresponding to 1952 when the first atmospheric deposition of ^{137}Cs took place can be determined. The penetration of ^{137}Cs is expected to be in the layers of 58–60 cm (RD-3), 32–34 cm (RD-6), 26–28 cm (RD-10) and 40–42 cm (RD-13). However the penetration of ^{137}Cs appears to be deeper than these layers.

Sediment inventories of ^{210}Pb$_{xs}$ and ^{137}Cs and sediment focusing/erosion factors

When sediment-laden river water is discharged into an impoundment, a majority of the sedimentary material is initially deposited in delta located at the river mouth and subsequently finer sedimentary particles are transported to farther distances from the river mouth within the impoundment. Thus, if excessive sediments deposit at the river mouth, we expect higher inventories of ^{210}Pb$_{xs}$ and ^{137}Cs. The finer sedimentary material transported by water movement also may contain higher specific activity due to surface area effect. The inventories of ^{210}Pb$_{xs}$ or ^{137}Cs (I_m^i in dpm cm^{-2}) in each of the cores were calculated from the following equation:

$$I_m^i = \sum_{i=1}^{n} (A_i \times m_i) \tag{3}$$

where m_i (g cm^{-2}) is the mass depth of 'i'th sediment layer and A_i is the activity (dpm/g) in the 'i'th layer of ^{210}Pb$_{xs}$ or ^{137}Cs. Inventories of ^{210}Pb$_{xs}$ and ^{137}Cs (Table 1) varied between 21.5 and 82.4 dpm cm^{-2} and 6.8 and 40.0 dpm cm^{-2}, respectively. Since the sedimentary record in Union Lake goes back to 87 y and the retrieval of cores seems incomplete in some of the cores (RD-1, 8 and 9; Fig. 3), the inventories of these cores are less than the others. The inventories of ^{210}Pb and ^{137}Cs are significantly higher in RD-3 than the rest of the cores.

The measured inventories of ^{210}Pb$_{xs}$ or ^{137}Cs in the sediment cores can be used to determine sediment focusing factors (F_f^i) by comparing the measured and expected inventories:

$$F_f^i = \frac{I_m^i}{I_{ex}^i} \tag{4}$$

where (I_{ex}^i) is the expected fallout inventory of ^{210}Pb$_{xs}$ or ^{137}Cs (dpm cm^{-2}). Note that there is additional erosional input of both ^{210}Pb and ^{137}Cs which needs to be taken into account. In smaller lakes with larger watershed area, this input could be quite significant. For example, McCall et al. (1984) observed that the total accumulation of ^{210}Pb$_{xs}$ and ^{137}Cs exceeds direct atmospheric loading between ~15% and ~80% in three reservoirs in northeastern Ohio, USA where the ratio of the drainage basin area/surface area of the lakes varied between 27 and 191 (McCall et al., 1984). For Union Lake, the ratio of the unimpounded subwatershed area upstream of Union Lake (616 km^2)/surface area of Union Lake (2.12 km^2) is ~290. Assuming a watershed residence time of ~3000 y for ^{210}Pb and ^{137}Cs (Smith et al., 1987), we could get ~3 times [=(290 * atmospheric deposition derived inventory) * 0.00033 (fractional annual input of ^{210}Pb or ^{137}Cs from the watershed) * mean-life of ^{210}Pb (or ^{137}Cs)] as that of the direct atmospheric deposition-derived inventory could come from the erosional input (similar calculation is given in Ravichandran et al., 1995). Note that ^{137}Cs is less particle-reactive with lower K_d values compared to ^{210}Pb. Although there is no ^{210}Pb annual depositional flux data for the study site, we can use the measured value in Detroit (42°25′ N; 83°1′ N) which is located at about 180 km away. The atmospheric

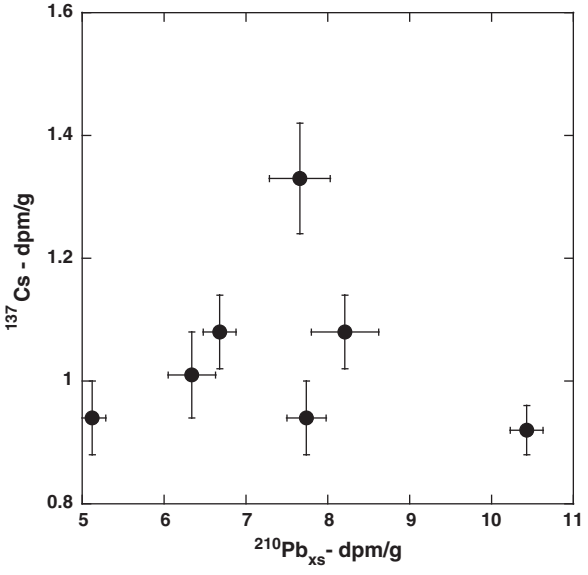

Fig. 2. ^{137}Cs activity versus ^{210}Pb$_{xs}$ activity in the upper 1 cm of the sediment cores.

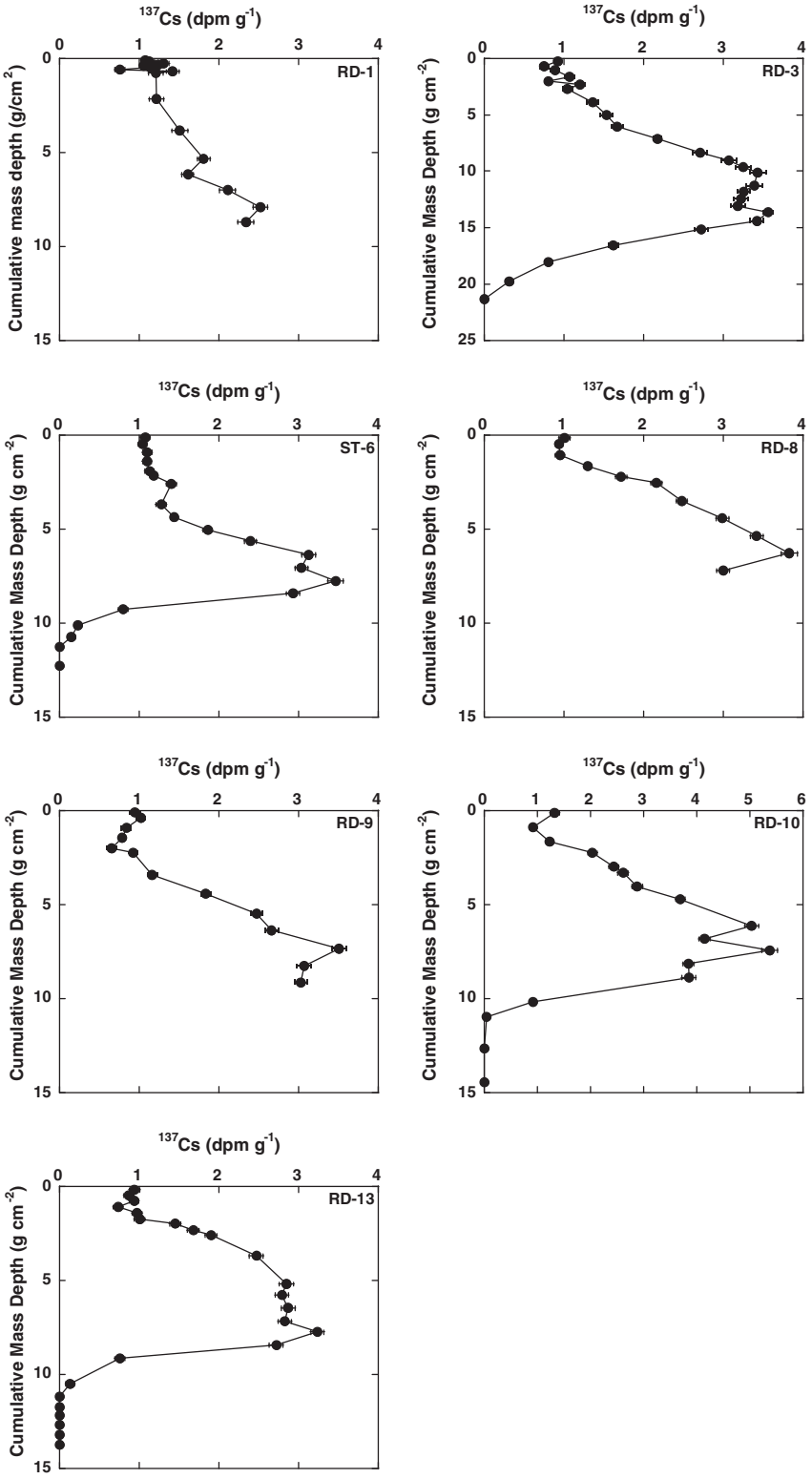

Fig. 3. Vertical profiles of ^{137}Cs. In cores RD-1, RD-8 and RD-9, only partial lengths of the full core were retrieved, based on ^{137}Cs vertical profiles. The bottom-most layer corresponding to 1923 is not expected to have ^{137}Cs (e.g., as found in RD-6, RD-10 and RD-13), if there is no post-depositional diffusion of ^{137}Cs.

depositional flux measured over a period of 18 months in Detroit was reported to be 1.56 dpm cm^{-2} y^{-1} (McNeary and Baskaran, 2003) which corresponds to 50.2 dpm cm^{-2} (= atmospheric depositional flux * mean-life of ^{210}Pb, 32.18 y). There is no direct atmospheric depositional flux data for ^{137}Cs. However, from the measured global fallout data for ^{90}Sr and the relationship between ^{137}Cs and ^{90}Sr, one can estimate the depositional flux of ^{137}Cs. The nearest city to Union Lake where time-series bomb fallout monitoring was conducted was in Argonne, IL. The 100-year precipitation average for Chicago is 83 cm and the average precipitation for Union City, MI is 94 cm and the latitudes are also comparable (Argonne 41.7°N). The measured inventory of ^{137}Cs for Argonne, IL is 3.27 dpm cm^{-2} (decay corrected to January

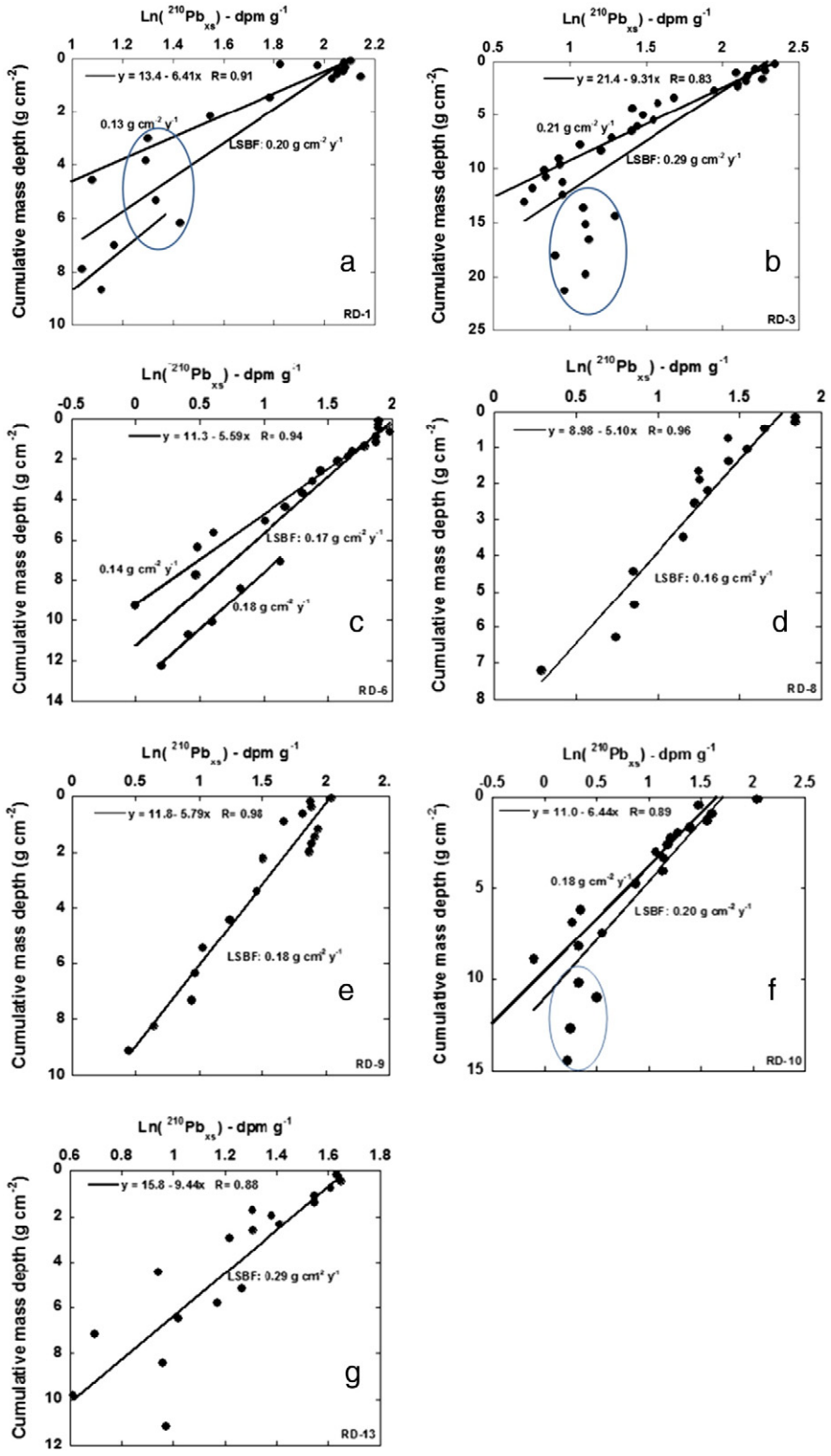

Fig. 4. Vertical distribution of Ln($^{210}Pb_{xs}$) for seven cores identified in lower right of each panel. In panels a), b), and f), the sediments within the ellipse are likely a result of flood event corresponding to 1952 when a relatively large amount of coarse-grained sediments were deposited. In a), b), c) and f) multiple lines are drawn, with and without data points which are likely influenced by the flood event. Equation in the upper portion of each panel is the uppermost regression line equation (without flood points) while sedimentation rates, g cm^{-2} y^{-1}, are given for individual lines without flood period or for all data points. LSBF indicates linear sedimentation rate using all data points.

1st, 2011), based on the $^{90}Sr/^{137}Cs$ (=1.5) relationship (HASL, 1977). The measured ^{137}Cs inventory is significantly higher than that of the direct overhead fallout. After the cessation of nuclear testing, the erosional input from the watershed continued to contribute to the lake.

The F_f^i values of >1.0 for $^{210}Pb_{xs}$ could also indicate sediment focusing. Of the 7 cores listed in Table 1, only one core (RD-3) has a value of 1.64, indicating that 64% excess ^{210}Pb is found and is likely due to sediment focusing (Table 1; note that the watershed erosional input could be ~3

Table 2
Linear sedimentation (LSR) and sediment accumulation rates (SARs) obtained using $^{210}Pb_{xs}$ and ^{137}Cs in sites from Union Lake, Michigan.

Core	$^{210}Pb_{xs}$-based Linear sed. rate ($cm\ y^{-1}$)	^{137}Cs-peak Linear sed. rate[a] ($cm\ y^{-1}$)	Sed. thickness based SAR[b] ($g\ cm^{-2}\ y^{-1}$)	$^{210}Pb_{xs}$-based SAR ($g\ cm^{-2}\ y^{-1}$)	^{137}Cs-peak SAR[ac] ($g\ cm^{-2}\ y^{-1}$)
RD-1	0.59	0.57	0.10	0.20	0.17
RD-3	0.98	1.04	0.26	0.28	0.29 (0.34)
RD-6	0.53	0.57	0.15	0.18	0.17 (0.18)
RD-8	0.40	0.36	0.086	0.16	0.13
RD-9	0.41	0.40	0.11	0.123	0.16
RD-10	0.56	0.45	0.17	0.20	0.16 (0.19)
RD-13	0.52	0.66	0.19	0.18	0.22 (0.22)

[a] ^{137}Cs-based LSR was obtained using ^{137}Cs peak (1963); LSR and SAR obtained for RD-1 are not reliable, as the peak of ^{137}Cs is uncertain and it is likely that it is below the bottom most layer collected. Based on the highest ^{137}Cs concentrations in RD-8 and 9, it seems likely that the highest concentration may represent the ^{137}Cs peak.
[b] Since the complete core was not recovered in RD-1, RD-8 and RD-9, we get significantly lower SAR for these three cores.
[c] Numbers in parenthesis denote SAR based on the appearance of ^{137}Cs, corresponding to 1952.

times higher the direct atmospheric depositional input and is not included in the calculation of I^i_{ex}). Although sediment focusing is not expected to affect the chronology when the focusing results in constant input of $^{210}Pb_{xs}$ to the sampling site (which implies the constant periodic addition of $^{210}Pb_{xs}$ to the sediments from the time the sediments deposited), the constant addition of transient tracer such as ^{137}Cs will affect the shape of ^{137}Cs, but not the horizon corresponding to the ^{137}Cs peak or its first introduction. Due to bottom topography and/or local currents, fine-grained sediments can be winnowed into areas of greater accumulation (Blais and Kalff, 1995; Crusius and Anderson, 1995; Wong et al., 1995; Jweda and Baskaran, 2011). In the remaining 6 sites, the F^i_f values for ^{210}Pb ranged between 0.43 and 0.74 (Table 1; note that the inclusion of erosional input will make this range of values between 0.11 and 0.19). As was mentioned before, the coring is partial in many of the cores (Fig. 4) and thus, F^i_f values are expected to be less than one. The F^i_f values for ^{137}Cs varied between 5.4 and 12.2 (Table 1; note that inclusion of erosional input will result in a range of values between 1.4 and 3.1), with the highest value in the same core where F^i_f value of ^{210}Pb was 1.64, again confirming that there is sediment focusing on this site. Although the atmospheric deposition of ^{137}Cs has been negligible since early 1970s, the input to the lakes are from both ^{137}Cs-laden suspended and bed load sediments, as well as dissolved ^{137}Cs (including colloidal). The fractional amount of ^{137}Cs derived from direct atmospheric deposition in sediment cores is relatively small, less than 25%, based on the four cores (RD-3, 6, 10 and 13) for which the ^{137}Cs level is found to be below detection limit at the bottom of the layer and a majority of the ^{137}Cs is derived from the erosional input.

The $^{210}Pb_{xs}/^{137}Cs$ inventory ratios in sediment cores were expected to be 15.2, if all ^{137}Cs and $^{210}Pb_{xs}$ were derived from atmospheric deposition. Although the atmospheric depositional flux patterns of ^{210}Pb (steady-state) and ^{137}Cs (transient state; ceased since early 1970s) are different, the annual watershed-derived fractional inventory of ^{210}Pb and ^{137}Cs is expected to be different for ^{137}Cs and ^{210}Pb due to differences in the particle affinity of Cs and Pb. In our sediment cores, this ratio varies between 0.99 and 2.39 indicating differential erosional input of Cs and Pb. The partitioning coefficient of ^{210}Pb is about 1 to 2 orders higher than that of ^{137}Cs in freshwater system (K_d (^{210}Pb) > K_d (^{137}Cs)), with much longer watershed residence time of ^{210}Pb compared to that of ^{137}Cs. Although most of the ^{210}Pb and ^{137}Cs were eventually derived from atmospheric deposition, because of the differences in the chemical affinities, the erosional input of these nuclides are expected to be different, with fractional erosional input flux of ^{137}Cs to be higher than that of ^{210}Pb (Smith et al., 1987; Smith et al., 2000; Jweda and Baskaran, 2011).

Sediment accumulation rates

In a system such as the dams that are less than 100 y old, there are four ways of determining the average SARs: i) using the vertical profiles of $^{210}Pb_{xs}$ and ^{137}Cs (based on ^{137}Cs peak (SAR = cumulative mass depth corresponding to peak ^{137}Cs / (year of sediment core collection − 1963)); ii) from the total thickness of soft sediments that deposited since the construction of the impoundment to the year of collection; iii) gage-based discharge of suspended particulate matter; and iv) from the trend line of sediment yield versus watershed drainage area. For the first time, we have compared the sedimentation rate obtained by all these different methods.

The vertical profiles of cumulative mass depth versus ln $^{210}Pb_{xs}$ plots are given in Fig. 5. To obtain the SARs using $^{210}Pb_{xs}$, three commonly-used models have been employed, depending on the constancy of the fluxes of sedimentary particles and ^{210}Pb. The first model was the constant-^{210}Pb flux: constant sedimentation model (CFCS-model, e.g., Robbins, 1978; Appleby and Oldfield, 1992). The second model was the constant rate of supply model (CRS), which assumes that the rate of supply of ^{210}Pb is constant, even if the sediment accumulation rate varies over time. Note that the atmospheric depositional flux is a function of the amount of precipitation in most regions, except in areas which are dominated by maritime air masses (such as some islands and coastal areas). Thus the atmospheric depositional flux is likely variable. The third model was the constant initial concentration (CIC) model which implies that even if the sediment flux varies, the atmospheric depositional flux will also co-vary to keep the specific activity constant (Robbins, 1978; Robbins and Edgington, 1975; Appleby et al., 1979; Appleby and Oldfield, 1992). Of these models, the CRS and CIC models have produced chronologies with limited success. Both CIC and CRS models did not yield reliable ages on sediment cores collected

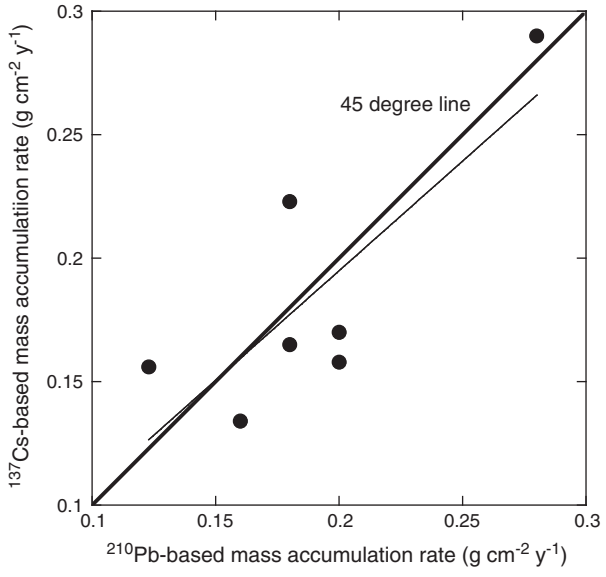

Fig. 5. Mass accumulation rate comparison – ^{137}Cs – versus $^{210}Pb_{xs}$ based. ^{137}Cs-based sediment accumulation rate is based on the ^{137}Cs peak. In three cores where the full core was not retrieved, the highest ^{137}Cs concentration is assumed to be the peak, although it is uncertain in cores RD-1, 8 and 9.

from Clinton River and Lake St. Clair while $^{210}Pb_{xs}$-based on CFCS-model and ^{137}Cs-peak based ages agreed very well (Jweda and Baskaran, 2011). Comparison of SARs from adjacent 3 lakes in Connecticut showed that in one Lake CIC model-based SAR was closer to ^{137}Cs-based SAR while in two other lakes, the CRS model-based SARs were closer to corresponding ^{137}Cs-based SARs (Benoit and Rozan, 2001). It appears that there is no consensus on the size of the lakes to the ^{210}Pb-model that is appropriate, although the changes in watershed erosional input are expected to affect larger lakes to a lesser extent. Also, in lakes where the watershed area/lake surface area ratio is low, the variations in sediment accumulation rates are more likely smaller. Union Lake is similar to the Lake St. Clair riverine–lacustrine system, and so we have used the CFCS model to calculate the SARs for the following reasons: i) the land use history analysis in the watershed area of Union Lake shows that the peak logging activity and peak agricultural activity had already occurred prior to the construction of the Riley Dam in 1923; and ii) there were two years when there were excessive flooding and in the rest of the years, the sediment discharge to the impoundment has likely remained relatively constant and thus it is reasonable to assume that the sedimentation rates also remained constant.

The $^{210}Pb_{xs}$ activity (A_d) at any depth 'd' can be calculated from the equation:

$$A_d = A_o e^{-\lambda_{Pb} t} \quad (5)$$

where A_d and A_o are the activities of $^{210}Pb_{xs}$ in a sediment layer at depth 'd' (cm) and at the surface layer (initial activity), respectively, and t is the age (y) of the sediment layer at depth 'd'. When the ln $^{210}Pb_{xs}$ activities are plotted against the cumulative mass depth, the resultant least squares best fit slope is used to calculate the mass accumulation rate (ω in g cm^{-2} y^{-1}):

$$\omega = \text{slope} \times (-\lambda_{Pb}). \quad (6)$$

Linear sedimentation rates (S, in cm y^{-1}) using $^{210}Pb_{xs}$ were calculated by plotting ln $^{210}Pb_{xs}$ activities against the linear depth and substituting ω for S in Eq. (6). Because the sediments undergo compaction, mass accumulation rates are always preferred over the linear sedimentation rates. Using the CFCS model, the sediment layer ages (y) can be calculated using the equation:

$$t_{CFCS} = \frac{M}{\omega} \quad (7)$$

where M is the cumulative mass depth (g cm^{-2}).

The mass accumulation rate calculated using Eq. (6) varied between 0.12 and 0.29 g cm^{-2} y^{-1} (Table 2). The ^{137}Cs-peak based mass accumulation rates (= mass depth where highest ^{137}Cs activity found / (year of collection of the core − 1963)) varied from 0.06 to 0.29 g cm^{-2} y^{-1}; note that the ^{137}Cs peaks are not clearly identified for cores RD-1, 8 and 9. Of these, the length of the core for RD-1 is not long enough to identify clear ^{137}Cs peak.

Discussion

Intercomparison of ^{137}Cs- and $^{210}Pb_{xs}$-based sediment accumulation rates

Excess ^{210}Pb-based methods have been widely used to date sediment cores from lakes. The $^{210}Pb_{xs}$-based chronology can be affected by a number of factors that include changes in the annual atmospheric depositional flux and erosional input, sediment focusing and erosion, post-depositional disturbances of sediment core by biological and/or physical mixing, ^{210}Pb produced from the discharge of groundwater containing high concentrations of ^{222}Rn and/or ^{226}Ra (e.g., Baskaran et al., 2014). Because of these factors, it has been strongly recommended that there should be one other method to validate the $^{210}Pb_{xs}$ chronology (Smith, 2001; Hancock et al., 2002). The SARs obtained by both $^{210}Pb_{xs}$ and ^{137}Cs-peak methods are compared to the SARs obtained using the total mass accumulated after impoundment construction (= total cumulative mass depth / (2010–1923)) in Table 2. Because there were no soft sediments prior to the construction of the dam, the total cumulative mass depth will yield an average sediment accumulation rate. As discussed earlier based on the vertical profiles of ^{137}Cs in some of the sediment cores (RD-1, 8, 9), the coring is incomplete and thus, the SARs in these cores are lower limits. However, in cores (RD-3, 6, 9 and 10) where the ^{137}Cs level reaches below detection limit, the SARs obtained from the cumulative mass depth are slightly lower (10–20%) than those obtained using $^{210}Pb_{xs}$ and ^{137}Cs-based methods.

The ^{137}Cs-based SAR is commonly based on one curve fitting method, based on the ^{137}Cs peak corresponding to 1963 (SAR = cumulative mass depth at ^{137}Cs-peak layer / (year of collection of the core − 1963), although the appearance of ^{137}Cs in sedimentary layer corresponding to 1952 can also be used as a time horizon. In sedimentary layers, if the year of appearance of ^{137}Cs, calculated based on either ^{137}Cs peak corresponding to 1963 or $^{210}Pb_{xs}$, agrees with the actual year of 1952, then, it is likely that the post-depositional diffusion of ^{137}Cs is negligible. Using the ^{137}Cs peak-based SAR, the bottom layers in 4 cores correspond to the following years: RD-3: 1939; RD-6: 1950; RD-10: 1955 and RD-13: 1940. In two out of 4 cores, the presence of ^{137}Cs is observed at depths corresponding to older than 1952. The deeper penetration depths could be due to the following reasons: i) during resuspension of surficial sediments some amount of ^{137}Cs could move downward; and ii) post-depositional diffusion of ^{137}Cs. While post-depositional migration of ^{137}Cs in lake sediment has been well-documented in literature from pore-water chemical data (^{137}Cs in pore water, K_d, K^+, NH_4^+, major cations, Fe and Mn, Evans et al., 1983; Comans et al., 1989), our purpose of the present study is focused on intercomparing the sediment accumulation rates obtained by excess ^{210}Pb and the one from ^{137}Cs (both 1963 peak and the first appearance of ^{137}Cs corresponding to 1952). Blais et al. (1995), from a synthesis of 31 dated cores by ^{210}Pb and ^{137}Cs from lakes in Norway, New England, northern Canada showed the presence of ^{137}Cs at ^{210}Pb-inferred dates before 1850 and they attributed to post-depositional migration of ^{137}Cs. There was very good agreement between ^{210}Pb-based and ^{137}Cs-based in hard water lakes (Michigan, Erie, and Ontario; Blais et al., 1995). From the simultaneous analysis of ^{137}Cs and ^{210}Pb from 16 lakes in Scandinavia and 14 lakes from northern New England, Davis et al. (1984) reported occurrence of ^{137}Cs at pre-fallout sediment depths and attributed this to downward molecular diffusion. In one sediment core from Lake St. Clair watershed, it was found that the ^{137}Cs penetration depth exceeded that of the excess ^{210}Pb and this was attributed to downward molecular diffusion of ^{137}Cs (Jweda and Baskaran, 2011). Without geochemical data in pore-water we will not be able to unequivocally address post-depositional migration of ^{137}Cs. However, earlier studies have attributed the presence of ^{137}Cs at pre-fallout depths to downward molecular diffusion (Davis et al., 1984; Blais et al., 1995; Jweda and Baskaran, 2011). Such diffusion would not shift the ^{137}Cs peak corresponding to 1963, but only will result in the broadening of the peak. The peak broadening could also arise from resuspension of the upper layer (~2 cm) (Benoit and Rozan, 2001) around 1963. In a recent study from a relatively small lake in southwestern Arkansas, it was shown that the peak ^{137}Cs corresponded to 1963 and the penetration depth of ^{137}Cs corresponded to 1952, indicating no post-depositional diffusion of ^{137}Cs. In that case the historical peak Hg levels arising from Hg mining in the region matched with the chronology obtained from ^{137}Cs, but the $^{210}Pb_{xs}$ profile did not decrease systematically with depth and this was attributed to major changes in the watershed (Baskaran et al., 2014).

While ^{137}Cs peak is widely used to obtain chronological information, the post-depositional sediment mixing due to physical and/or biological mixing, and diffusion could result in peak broadening, but unlikely it will result in peak shifting. Similar to many advection and diffusion transport processes in surface waters, the peak will result in broadening and thereby increase in the standard deviation in the shape of the peak

(discussion below). The ^{137}Cs-based SAR (Fig. 6) is plotted against the $^{210}Pb_{xs}$-based SAR and there is an overall positive correlation. In all of the cores, the difference between these two nuclides-based methods is less than ±15%.

Characterization of the ^{137}Cs peak to obtain information on the sediment mixing and ^{137}Cs diffusion

If all the ^{137}Cs in a sediment core are derived from direct atmospheric deposition, then, the ^{137}Cs vertical profile should be identical to the historical atmospheric fallout curve for ^{90}Sr (Fig. 6), which is a near-ideal Gaussian distribution. This is under the assumption that the atmospherically-delivered ^{137}Cs is removed from the water column to the sediments quickly. Because the K_d of Cs in freshwater is high (~10^5 cm^3/g, e.g., Edgington and Robbins, 1990), this assumption is reasonable. The shape of the ^{137}Cs likely provides insight on sediment resuspension and vertical sediment mixing (e.g., Baskaran et al., 2014). Details on the basic characteristics of a Gaussian curve relevant to the ^{137}Cs fallout peak are given in Baskaran et al. (2014). The mixing coefficient and the standard deviation of ^{137}Cs distribution are likely related when the physical and/or biological mixing alters the upper sedimentary layer. From the property of the Gaussian distribution curve, the amount of sediments lying within one standard deviation (σ) on either side of the point of maximum ^{137}Cs concentration includes 68% of the total ^{137}Cs in the sediment core. The ^{137}Cs concentration at 1 σ from the point of maximum concentration equals the maximum concentration multiplied by 0.61 (Hemond and Fechner, 2015). The 1σ for ^{90}Sr fallout peak corresponds to ±0.95 y while for the measured ^{137}Cs profiles, the 1σ values are: RD-3: ±12.5 y; RD-6: ±8.5 y; RD-10: ±13.1 y; and RD-13: ±11.5 y. The years were calculated from the vertical profiles of ^{137}Cs and by taking the values of ^{137}Cs-based SAR given in Table 2. These large σ values for the measured ^{137}Cs vertical profiles are likely due to post-depositional physical mixing of sediments from resuspension. It is likely that diffusion of ^{137}Cs could also contribute to the peak broadening.

Variations of spatial and temporal sediment accumulation rates

Analysis of land use history in the watershed area of Union Lake shows that the peak of logging activity and the peak of agricultural activity had already occurred prior to the construction of the Riley Dam in 1923. The amount of autochthonous source of sediments such as from productivity is likely negligible, as evidenced by the total organic carbon (<2%) in the upper surficial sediments (data unpublished). If the amount of water and sediment discharge remained constant since the construction of the dam, then, it is likely that the sediment delivery to the Union Lake and sedimentation rates in most areas of the lake have remained constant. However, in years when there is large flooding, higher sediment transport loads and higher SARs are expected in those layers corresponding to these flood events. Those flood events from the historical records can be validated using ^{210}Pb and ^{137}Cs-based chronology. Based on a variety of historical records, it seems that there were no historical events that would alter the sedimentation record of the Union Lake except the flooding recorded at the St. Joseph River downstream of Union Lake in 1950 and 1982 (FEMA, 2010).

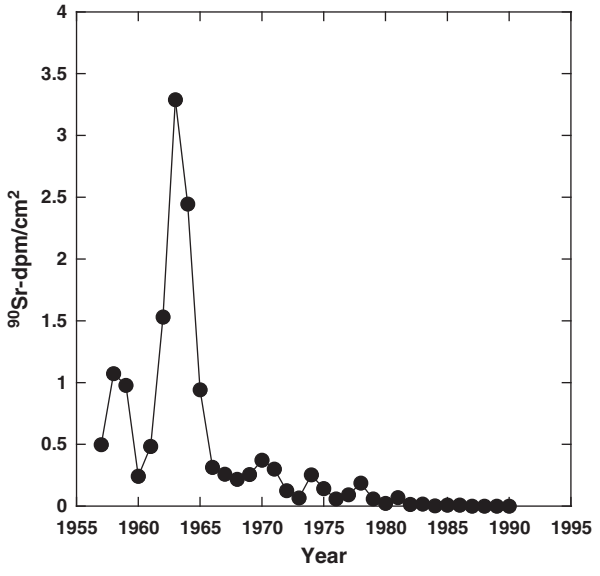

Fig. 6. Fallout record of ^{90}Sr in Argonne, IL.
Data taken from Environmental Measurements Laboratory-DOE data.

A plot of $^{210}Pb_{xs}$-based sediment accumulation rate from the river mouth to the end (from north to south, Fig. 1) does not show any relationship in contrast to what is expected. As the sediments are discharged in the river mouth, we expect a gradient in the SAR, with the highest SAR near river mouth and the lowest farthest from the water discharge area. It is also likely that ^{137}Cs-bearing sediment resuspension at the margins of Union Lake depositional basin could result in sediment focusing. It has been shown in Lake Michigan that the cores collected at the margins of the depositional areas showed losses of sediment while those collected from within the basins was found to have gained ^{137}Cs-laden sediments (Edgington and Robbins, 1990). However, if majority of the sediments delivered at the mouth of the river are mud fraction and can be carried to farther distances, it will likely result in uniform deposition. The bottom currents and the advection of water movement result in relatively uniform distribution of sediments.

During major flood events, large amounts of sediments would accumulate within the delta and throughout the impoundment which could serve as a signature and provide independent validation of the radionuclide-based chronology. As presented earlier, the ^{226}Ra concentrations in sedimentary layers corresponding to flood events can be seen in RD-10 and RD-13 cores which were collected near the river mouth. In RD-13, 40–42 cm corresponds to 1951, assuming sedimentation accumulation rate of 0.223 g cm^{-2} y^{-1} (based on ^{137}Cs-peak, the corresponding $^{210}Pb_{xs}$-based value is 0.18 g cm^{-2} y^{-1}) and likely represents the 1952 flood event. In RD-10, the layer 30–32 cm corresponds to 1955, and 34–36 cm corresponds to 1947, taking 0.20 g cm^{-2} y^{-1} as the average sediment accumulation rate, and both of these samples have the lowest ^{226}Ra concentration, again indicating the presence of a coarser-grain material which was deposited from the 1952 flood event. In RD-6, the lowest ^{226}Ra concentration at 32–34 cm corresponds to 1954, using $^{210}Pb_{xs}$-based SAR of 0.18 g cm^{-2} y^{-1} and thus appears to be from the 1952 flood event. There are no other indications of low ^{226}Ra in any other layers. We do not see any major changes in the Ra or ^{210}Pb profiles due to 1980 flooding event and we presume the 1980 event is significantly smaller when compared to 1952 flood event.

Intercomparison of sediment accumulation rates obtained using five different methods

Of the five methods (two radionuclide based, sediment thickness based, sediment discharge based on gage data, and sediment yield curve-based, developed by US Army Corps of Engineers) utilized to determine sediment accumulation rates, one method provides a rough estimate of sediment loading (sediment yield curve-based). Using the regression equation obtained from a plot of sediment yield (tons/year) versus watershed drainage area (mi^2) for 61 data points from Great Lakes watersheds and Reservoirs, Creech et al. (2011) obtained a relationship:

$$Y(\text{sediment yield, tons/y}) = 407.3 * A^{0.77}(\text{watershed drainage area, sq. miles}) \times \left(r^2 = 0.78, n = 61\right).$$

With respect to the Union Lake, the impounded area (which is the watershed drainage area that is impounded) consists of 6.42×10^8 m^2 (248 mi^2), and the sediment yield estimated from the above equation corresponds to 2.58×10^{10} g/y (2.84×10^4 tons/y). For the surface area of the impounded lake of 2.12×10^6 m^2 (=525 acres) and assuming a uniform sediment accumulation throughout the Union Lake and a 100% sediment trapping efficiency, it corresponds to a mass accumulation rate of 1.2 g cm^{-2} y^{-1}, which is about 6 times higher than that obtained using $^{210}Pb_{xs}$ and ^{137}Cs-based values. However, it is quite likely that the sediment trapping is less than 100% in which case the sediment yield curve is an overestimate of the actual sediment accumulation rate. When sediments undergo deposition, some remineralization takes places in which Fe/Mn-oxides can undergo dissolution and a finite fraction of the organic matter can also undergo remineralization. Unlike in open oceans where most of the particles are biogenic and >90% of the recently-deposited sediments undergo remineralization and only less than 10% of the deposited sediments eventually undergoes burial and become historic record, in freshwater system where a majority of the sediments are terrigenous it is unlikely that a major portion of the sediments will undergo remineralization. Using the sediment accumulation rates obtained using ^{210}Pb and ^{137}Cs, one can get an empirical relation between the sediment yield and watershed drainage area. The sediment loads to the study areas can also be estimated using the High Impact Targeting 2.0 (HIT model) (Renard et al., 1996). The HIT model calculates the sediment loading by determining the sediment yield from the Universal Soil Loss Equation and determining the percentage of the soil delivered to the stream using the Spatially Explicit Delivery Model. Using the HIT model, sediment to the Union Lake was estimated to be 24,926 tons/y, corresponding to 1.1 g cm^{-2} y^{-1}. This model likely overpredicts the sediment loadings as it does not include storage of sediment in upstream reservoirs.

Finally, the St. Joseph River has a sediment gage upstream of the Union Lake as well as a flow gage downstream of the reservoir. Within the Union Lake subwatershed boundary, there are numerous additional dams that are constructed and hence the unimpounded watershed area represents the 'true drainage area' for the Union Lake. One can estimate the sediment accumulation rates based on the sediment gage data for both the unimpounded (516 mi^2) and impounded (248 mi^2) area of the watershed. From the estimated sediment discharges of 6384 tons/y for un-impounded area of the gages and 4811 tons/y for impounded area of the gages, we estimate mass accumulation rates of 0.28 g cm^{-2} y^{-1} and 0.21 g cm^{-2} y^{-1}, respectively which is in very good agreement with the radionuclide-based SARs.

Conclusions

This study of sediment retention characteristics of Union Lake has relevance to hundreds of reservoirs in the Great Lakes watershed. Impoundment removal is happening across the Great Lakes watersheds at a quickening pace and this removal has a direct impact on the sediment delivery to the Great Lakes. Lessons learned from the intercomparison of radioisotope-based dating method with those of other three methods discussed in this article have direct relevance to larger lakes, as the sedimentary record of the larger lakes go far beyond ~100 y and thus such intercomparison is not possible in larger lakes. From the ^{137}Cs and ^{210}Pb analysis of 7 sediment cores from Union Lake (impoundment constructed in 1923) in Michigan, USA and comparing the radionuclide-based sediment accumulation rates (or linear sedimentation rate) to that obtained from three other methods (total length of the core, sediment yield curve and sediment discharge measured using gages), the following conclusions are drawn:

i) The $^{210}Pb_{xs}$ sediment accumulation rates varied between 0.12 and 0.28 g cm^{-2} y^{-1} (peak ^{137}Cs-based: 0.13 to 0.29 g cm^{-2} y^{-1}) across the Union Lake, with no systematic variation from the river mouth to the end or with depth;
ii) The linear sedimentation rates based on $^{210}Pb_{xs}$, ^{137}Cs and bathymetric method generally agree;
iii) The vertical profiles of ^{137}Cs indicate if the vibra-coring collected the entire soft sediment core or only partial length of the core. The shape of the ^{137}Cs peak corresponding to 1963 peak is quantified for the first time to assess the extent of sediment mixing (biological and/or physical mixing) and diffusion by comparing with the global fallout curve;
iv) The sediment accumulation rates (1.2 g cm^{-2} y^{-1}) based on sediment yield curve is ~6 times higher than the average SAR obtained using radionuclides;
v) The average SAR obtained using the sediment load discharge gage data (0.21 g cm^{-2} y^{-1}) agrees well with the average SAR obtained using $^{210}Pb_{xs}$ and ^{137}Cs; and
vi) In this well-constrained system in terms of historical land use changes, amount of precipitation and sediment discharge data, we can identify the impact of flood event on the vertical profiles of $^{210}Pb_{xs}$ and ^{226}Ra.

Supplementary data to this article can be found online at http://dx.doi.org/10.1016/j.jglr.2015.03.013.

Acknowledgments

We thank a large number of people who assisted with various aspects of this project that include Pranesh Jayakumar and a large number of undergraduate students. We thank Editor-in-Chief Robert Hecky for providing insights on the relevance of this study to larger lakes. This project was funded by the U.S. Army Corps of Engineers (W911XK-10-C-0011 and W911XK-14-C-0023).

References

Appleby, P.G., Oldfield, F., 1992. Application of lead-210 to sedimentation studies. In: Ivanovich, M., Harmon, R.S. (Eds.), Uranium-series Disequilibrium: Applications to Earth, Marine and Environmental Sciences. Clarendon Press, Oxford, pp. 731–778.
Appleby, P.G., Oldfield, F., Thomson, R., Huttunen, P., Tolonen, K., 1979. ^{210}Pb dating of annually laminated lake sediments from Finland. Nature 280, 53–55.
Baskaran, M., Naidu, A.S., 1995. ^{210}Pb-derived chronology and the fluxes of ^{210}Pb and ^{137}Cs isotopes into continental shelf sediments, East Chukchi Sea, Alaskan Arctic. Geochim. Cosmochim. Acta 59, 4435–4448.
Baskaran, M., Nix, J., Kuyper, C., Karunakara, N., 2014. Problems with the dating of sediment core using excess ^{210}Pb in freshwater system impacted by large scale watershed changes. J. Environ. Radioact. 138, 355–363.
Benoit, G., Rozan, T.F., 2001. ^{210}Pb and ^{137}Cs dating methods in lakes: a retrospective study. J. Paleolimnol. 25, 455–465.
Blais, J.M., Kalff, J., 1995. The influence of lake morphometry on sediment focusing. Limnol. Oceanogr. 40, 582–588.
Blais, J.M., Kalff, J., Cornett, R.J., Evans, R.D., 1995. Evaluation of ^{210}Pb dating in lake sediments using stable Pb, *Ambrosia* pollen, and ^{137}Cs. J. Paleolimnol. 13, 169–178.
Comans, R.N.J., Middelburg, J.J., Zonderhuis, J., Woittiez, J.R.W., De Lange, G.J., Das, H.A., Van Der Weijden, C.H., 1989. Mobilization of radiocesium in pore water of lake sediments. Nature 339 (6223), 367–369.
Comer, P.J., Albert, D.A., 1998. Vegetation of Michigan Circa 1800. Michigan Natural Features Inventory, Lansing (2 maps).
Creech, C.T., Selegean, J.P., Dahl, T.A., 2010. Historic and modern sedimentary yield from a forested watershed and its impact to navigation. Paper Presented at the 2nd Joint Federal Interagency Conference, Los Vegas, NV.
Creech, C.T., et al., 2011. Riley Reservoir Sedimentation Study, Union City, Michigan.
Crusius, J., Anderson, R.F., 1995. Sediment focusing in six small in six small lakes inferred from radionuclide profiles. J. Paleolimnol. 13, 143–155.
Crusius, J., Bothner, M.H., Sommerfeld, C.K., 2004. Bioturbation depths, rates and processes in Massachusetts Bay sediments inferred from modeling of ^{210}Pb and $^{239+240}Pu$ profiles. Estuar. Coast. Shelf Sci. 61, 643–655.
Davis, R.B., Hess, C.T., Norton, S.A., Hanson, D.W., Hoagland, K.D., Anderson, D.S., 1984. ^{137}Cs and ^{210}Pb dating of sediments from soft water lakes in New England (USA) and Scandinavia, a failure. Chem. Geol. 44, 151–185.
Edgington, D.N., Robbins, J.A., 1990. Time scales of sediment focusing in large lakes as revealed by measurement of fallout Cs-137. In: Tilzer, M.M., Serruya, C. (Eds.), Large Lakes: Ecological Structure and Function. Springer-Verlag, New York, pp. 210–223.
Evans, D.W., Alberts, N.N., Clark, R.A., 1983. Reversible ion-exchange fixation of cesium-137 leading to remobilization from reservoir sediments. Geochim. Cosmochim. Acta 47, 1041–1049.
FEMA (Federal Emergency Management Agency), 2010. Federal Insurance Administration, Flood Insurance Study, St. Joseph County, Michigan, Washington, D.C. (June 4).

Fuller, C.C., A. A., vanGeen, Baskaran, M., Anima, R., 1999. Sediment chronology in San Francisco Bay, California, defined by ^{210}Pb, ^{234}Th, ^{137}Cs, and $^{239, 240}$Pu. Mar. Chem. 64, 7–27.

Hancock, G., Edgington, D.N., Robbins, J.A., J.N. Smith, J.N., G. Brunskill, G., Pfitzner, J., 2002. Workshop on radiological techniques in sedimentation studies: methods and applications. In: Fernandez, J.M., Fichez, R. (Eds.), Environmental Changes and Radioactive Tracers. Proceedings of the South Pacific Environmental Radioactivity Association (SPERA) 2000. IRD Editions, Paris (532 pp.).

HASL, 1977. Final Tabulation of Monthly Sr-90 Fallout Data: 1954–1976, Health and Safety Laboratory-329. Energy Research and Development Administration.

Hemond, H.F., Fechner, E.J., 2015. Chemical Fate and Transport in the Environment. third ed. Academic Press, New York.

Hossain, F., Jeyachandran, I., Pielke, R., 2009. Have large dams altered extreme precipitation patterns? Eos 90 (48), 452–453 (1st December).

Jweda, J., 2008. Short-lived Radionuclides (^{210}Pb, ^{7}Be and ^{137}Cs) as Tracers of Particle Dynamics and Chronometers for Sediment Accumulation and Mixing Rates in a River System in Southeast Michigan. Department of Geology, Wayne State University, Detroit, MI, p. 167.

Jweda, J., Baskaran, M., 2011. Interconnected riverine–lacustrine systems as sedimentary repositories: case study in southeast Michigan using excess ^{210}Pb and ^{137}Cs-based sediment accumulation and mixing models. J. Great Lakes Res. 37, 432–446.

McCall, P.L., Robbins, J.A., Matisoff, G., 1984. ^{137}Cs and ^{210}Pb transport and geochronologies in urbanized reservoirs with rapidly increasing sedimentation rates. Chem. Geol. 44, 33–65.

McNeary, D., Baskaran, M., 2003. Depositional characteristics of ^{7}Be and ^{210}Pb in Southeastern Michigan. J. Geophys. Res. 108 (D7). http://dx.doi.org/10.1029/2002JD003021 (15 pages, 4210,).

National Inventory of Dams, 2010. http://geo.usace.army.mil/.

Ravichandran, M., Baskaran, M., Sanstschi, P.H., Bianchi, T.S., 1995. Geochronology of sediments in the Sabine–Neches estuary, Texas, U.S.A. Chem. Geol. 125, 291–306.

Renard, K., Foster, G., Weesies, G., McCool, D., Yoder, D., 1996. Predicting soil erosion by water: a guide to conservation planning with the Revised Universal Soil Loss Equation (RUSLE). Agriculture Handbook Number 703. USDA.

Ritchie, J.C., McHenry, J.R., 1990. Application of radioactive fallout cesium-137 for measuring soil erosion and sediment accumulation rates and patterns: a review. J. Environ. Qual. 19, 215–233.

Robbins, J.A., 1978. Geochemical and geophysical applications of radioactive lead isotopes. In: Nriagu, J.O. (Ed.), Biochemistry of Lead. Elsevier, Amsterdam, pp. 285–393.

Robbins, J.A., Edgington, D.N., 1975. Determination of recent sedimentation rates in Lake Michigan using Pb-210 and Cs-137. Geochim. Cosmochim. Acta 39, 285–304.

Robbins, J.A., Mudrock, A., Oliver, B.G., 1990. Transport and storage of ^{137}Cs and ^{210}Pb in sediments of Lake St. Clair. Can. J. Fish. Aquat. Sci. 47, 572–587.

Smith, J.N., 2001. Why should we believe ^{210}Pb sediment geochronologies? J. Environ. Radioact. 55, 121–123.

Smith, J.N., Ellis, K.M., Nelson, D.M., 1987. Time-dependent modelling of fallout radionuclide transport in a drainage basin: significance of "slow" erosional and "fast" hydrological components. Chem. Geol. 63, 157–180.

Smith, J.N., Comans, R.N.J., Ireland, D.G., Nolan, L., Hilton, J., 2000. Experimental and in-situ study of radiocesium transfer across the sediment–water interface and mobility in lake sediments. Appl. Geochem. 15, 833–848.

Wong, C.S., Sanders, G., Engstrom, D.R., Long, D.T., Swackhamer, D.L., Eisenreich, S.J., 1995. Accumulation, inventory, and diagenesis of chlorinated hydrocarbons in Lake Ontario sediments. Environ. Sci. Technol. 29, 2661–2671.

World Bank, 1998. Sustainability of Dams–Reservoir Sedimentation Management and Safety Implications.